Theoretical study and wavefunction analysis of cyclo[18]carbon-benzene dimer

Peng Fu

State Key Laboratory of Superhard Materials，College of physics，Jilin University，Changchun 130012，China

Shenzhen Research Institute, Jilin University, Shenzhen 518057, China

Abstract

The structural optimization and vibration analysis of a bimolecular composed of cyclo[18]carbon and benzene are carried out by using the density functional theory based ωB97X-D3/def2-TZVP. Then based on the optimized structure, interaction energy with counterpoise correction were calculated at the ωB97X-V/def2-QZVPP level. Analyze Mayer bond order, orbital composition and weak interactions, drawn infrared spectrum, Raman, Density-of-States(DOS) and weak interaction diagram. The PSI4 software used to characterize the nature of intermolecular interaction. For the first time, we have theoretically studied the interaction between the cyclo[18]carbon and the benzene ring, providing theoretical guidance for the practical application of the cyclo[18]carbon in reality.

Keywords

Cyclo[18]carbon、Benzene、Theoretical calculation、Wavefunction analysis

1. Introduction

Carbon, as one of the elements with the most allotropes, people have discovered various new carbon materials like graphyne[1], penta-graphene[2], T-carbon[3-4] in recent years based on theoretical research. As one of the most exciting research achievements in this field, cyclo[18]carbon has received widespread attention[5-7] since its synthesized in the experiment in 2019[8]. In fact, before it was experimentally synthesized, theoretical research had been conducted on it as early as 1966[9], people have made unremitting efforts to synthesize it and predicted a series of its properties through theoretical calculations, the research on it was even more explosive after it was synthesized[10-12].

We realize that its characteristics of interaction with other molecule may be significantly different from general chemical systems due to the unusual geometric configuration and electronic structure of the cyclo[18]carbon, currently, only few studies have discussed the interaction between cyclo[18]carbon and small molecule, among them, the work of liu and lu are the relatively representative[13-18], most of them have studied the interactions between cyclo[18]carbon and other systems, interaction between multiple molecules in system actually very important for the practical application of a chemical substance. And benzene ring is also one of the important cyclic molecules, It's very fascinating that we are curious about what kind of interaction will occur between cyclo[18]carbon and benzene ring, they are almost circular in shape, this may have significant implications for the application of the complex of cyclo[18]carbon and benzene ring that cannot be ignored, its interaction with cyclo[18]carbon has not been studied yet.

In this paper, we will first explore the dimer structure formed by cyclo[18]carbon and benzene ring, and conducted bond order analysis on it. Then we drawn the infrared and Raman spectral of the dimer, indicate the corresponding relationship between its vibration mode and several peaks in spectral. Finally, we analyzed its molecular orbital composition and weak interaction, this has

potential significance for exploring the adsorption of cyclo[18]carbon and benzene ring in the long run.

2. Method

We constructs the molecular geometric model of cyclo[18]carbon-benzene dimer by GaussView6.0[19] software, Geometry optimizations and frequency analyses were implemented by ORCA[20] program using ωB97X-D3[25] functional in conjunction with def2-TZVP[26] basis set, and the RIJCOSX technique[21-24] was enabled for accelerating the calculations, until the result converges. The comparative test of functionals in reference shows that ωB97XD[27] combined with def-TZVP[28] basis set can reasonably describe the geometry of Structure containing cyclo[18]carbon, Because all computing work was based on ORCA, But ORCA does not support ωB97XD, So we chose ωB97X-D3 that is similar to ωB97XD, It also applies to such a conjugated system[5]. Interaction energy with counterpoise correction were calculated by ORCA program using ωB97X-V[29] functional in conjunction with def2-QZVPP[26] basis set. We described the structure of cyclo[18]carbon-benzene dimer. Then, the wave function analysis software Multiwfn[30] was used to analyze Mayer bond order[31], Orbital composition and weak interactions, Drawn infrared spectrum, Raman, Density-of-States(DOS)and weak interaction diagram. Finally, the PSI4[32] software was used to implemented Symmetry-Adapted Perturbation Theory(SAPT)[33] to characterize the nature of intermolecular interaction, compare with the research results of cyclo[18]carbon dimer.

3. Results and discussion

3.1 structure and Mayer bond order analysis

We placed benzene ring inside cyclo[18]carbon as the initial structure before calculation, the plane where benzene ring was located was parallel to the plane where cyclo[18]carbon was located, and the center of benzene ring coincided with the center of cyclo[18]carbon, the initial structure is drawn in Fig.1. After calculation, we obtained stable structure without imaginary frequency, benzene ring has left its initial position due to a mismatch in size with cyclo[18]carbon, and benzene ring and cyclo[18]carbon are no longer parallel, the angle of two planes is 17°51′27″ as shown in Fig.2.

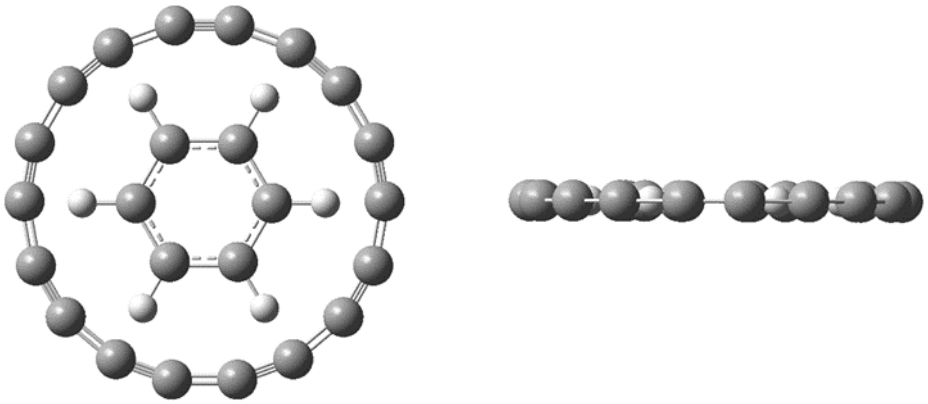

Fig.1 bird-view and cross-section view of initial structure

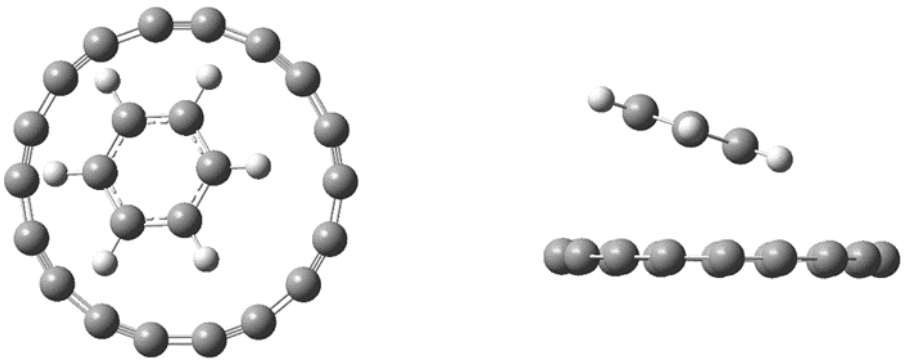

Fig.2 bird-view and cross-section view of optimized structure

The bonding of cyclo[18]carbon has been receiving much attention. The current research results indicated the C-C bond length in cyclo[18]carbon presents alternating characteristics, but it's not simply alternating single and triple bonds[5]. So, would the C-C bond in the cyclo[18]carbon still maintain alternating characteristics in the optimized cyclo[18]carbon-benzene dimer? We listed C-C bond length of cyclo[18]carbon and cyclo[18]carbon-benzene dimer in Table.1

Table 1 A: length of C-C in cyclo[18]carbon, B: length of C-C in cyclo[18]carbon-benzene dimer

Bond	Length A(Å)	Length B(Å)	Bond	Length A(Å)	Length B(Å)
1C-2C	1.22105	1.21638	10C-11C	1.34378	1.35357
2C-3C	1.34375	1.35294	11C-12C	1.22110	1.21659
3C-4C	1.22109	1.21623	12C-13C	1.34377	1.35363
4C-5C	1.34382	1.35279	13C-14C	1.22112	1.21645
5C-6C	1.22111	1.21619	14C-15C	1.34384	1.35362
6C-7C	1.34383	1.35293	15C-16C	1.22112	1.21656
7C-8C	1.22110	1.21634	16C-17C	1.34379	1.35360
8C-9C	1.34379	1.35328	17C-18C	1.22110	1.21650
9C-10C	1.22110	1.21650	18C-1C	1.34378	1.35331

We found that after optimizing cyclo[18]carbon-benzene dimer, C-C bond still maintain alternating characteristics in the optimized cyclo[18]carbon-benzene dimer, but the bond length has changed, long C-C bonds are longer, short C-C bonds are shorter, the change in length is within 0.01 Å. As an effective method of chemical bond analysis, bond order analysis is often used in bond formation analysis. The Mayer bond order is the most commonly used bond order, it's close to the actual bond order numerically. In physical nature, Mayer bond order reflects the electronic logarithm shared between two atoms. The Mayer bond orders of C-C bond in cyclo[18]carbon-benzene dimer were analyzed, and compare with C-C bond in cyclo[18]carbon in Table.2

Table 2 A: Mayer bond order of C-C in cyclo[18]carbon B: Mayer bond order of C-C in cyclo[18]carbon-benzene dimer

Bond	Value A	Value B	Bond	Value A	Value B
1C-2C	2.27373973	2.85785787	10C-11C	1.61123349	1.17049574
2C-3C	1.61114925	1.20588955	11C-12C	2.27385373	2.80415699
3C-4C	2.27370273	2.77581997	12C-13C	1.61075032	1.18631233
4C-5C	1.61081211	1.13852720	13C-14C	2.27396112	2.60256876
5C-6C	2.27392463	2.75984520	14C-15C	1.61069369	1.09971165
6C-7C	1.61072760	1.12751734	15C-16C	2.27405044	2.60321247
7C-8C	2.27380992	2.67455893	16C-17C	1.61056500	1.10427667
8C-9C	1.61092283	1.13576522	17C-18C	2.27397799	2.67124200
9C-10C	2.27382783	2.75894652	18C-1C	1.61120874	1.18830962

The calculation results of bond order also reflect a phenomenon, strong C-C bonds have become stronger, weak C-C bonds become even weaker.

3.2 IR and Raman spectral analysis

We simulated infrared (IR) in order to helps experimental chemists to judge the existence of cyclo[18]carbon-benzene dimer by comparing the spectra, the harmonic frequencies calculated at ωB97X-D3/def2-TZVP were scaled by 0.975 to approximately eliminate systematical error due to the harmonic approximation[34]. The value of FWHM is 8cm^{-1}, The current structure has two kinds of vibrations, namely in-plane and out-of-plane vibrations, they are highlighted as red and green spikes in the Fig.3, as shown in the Fig.3, the main kinds of vibrations are out-of-plane vibrations, while most of out-of-plane vibrations are concentrate in low wavenumber region, this phenomenon indicates that most of out-of-plane vibrations in cyclo[18]carbon-benzene dimer correspond to flexible motion, This is basically consistent with individual cyclo[18]carbon. There are four relatively intensive IR peaks, the corresponding vibrational coordinates are shown as insets of the Fig.3. The first one is at 517.0cm^{-1} and corresponds to alternating oscillation of long and short C-C bonds in cyclo[18]carbon, the second and fourth are in 701.1cm^{-1} and 3213.9cm^{-1}, corresponds to oscillation of hydrogen atoms and stretching of C-H bonds in benzene ring, respectively, the third one is at 2269.6cm^{-1} and corresponds to stretching of C-C bonds in cyclo[18]carbon. The blue and green curve in Fig.3 represent the contributions of benzene ring and cyclo[18]carbon, respectively, this can be confirmed by insets of the Fig.3. But two peaks of cyclo[18]carbon are slightly different compared to individual cyclo[18]carbon[5], this is because the cyclo[18]carbon we are studying is located in the composite structure, therefore, its peak position has been affected.

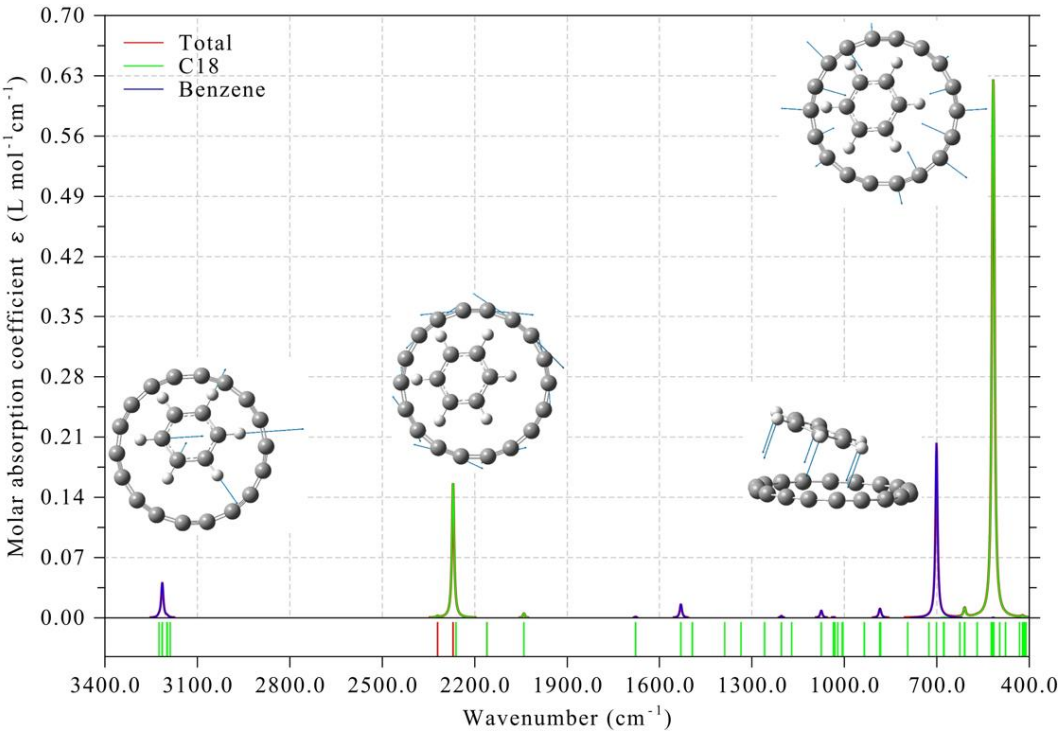

Fig.3 Simulated infrared (IR) spectrum of cyclo[18]carbon-benzene dimer, The red curve corresponds to molar absorption coefficient, blue and green curve represent the contributions of benzene ring and cyclo[18]carbon, The red and green spikes at bottom of the map indicate frequencies of in-plane and out-of-plane vibrational modes, respectively.

Then we also simulated Raman spectrum of cyclo[18]carbon-benzene dimer at the same calculation level, here is a worth noting, Raman intensity required for simulated Raman spectrum is not directly outputted by ORCA, but converted from Raman activity with temperature is 298.16K and incident light wavelength is 1064nm by using the following formula[16], S_i, I_i, and υ_i represent Raman activity, Raman intensity, and vibration frequency(wave number), respectively. υ_i represent frequency of incident light(wave number), T is temperature, h is planck constant, c is velocity of light, K is Boltzmann constant, C is unimportant constant. The 1064nm wavelength corresponds to the common Raman source Nd:YAG laser. It can be seen that there are two strong Raman peaks from Fig.4, which are respectively at a slightly high wavenumber 516.9cm^{-1} and a very low wavenumber 6.4 cm^{-1}, the higher one corresponds to alternating oscillation mode of long and short C-C bonds in cyclo[18]carbon, the lower one corresponds to oscillation mode of hydrogen atoms, as shown in the inset of Fig. 4, the IR spectrum and Raman spectrum of the cyclo[18]carbon-benzene dimer show evident complementary feature to each other.

$$I_i = \frac{C(\nu_0 - \nu_i)^4 S_i}{\nu_i B_i} \qquad B_i = 1 - \exp(-\frac{hc\nu_i}{KT})$$

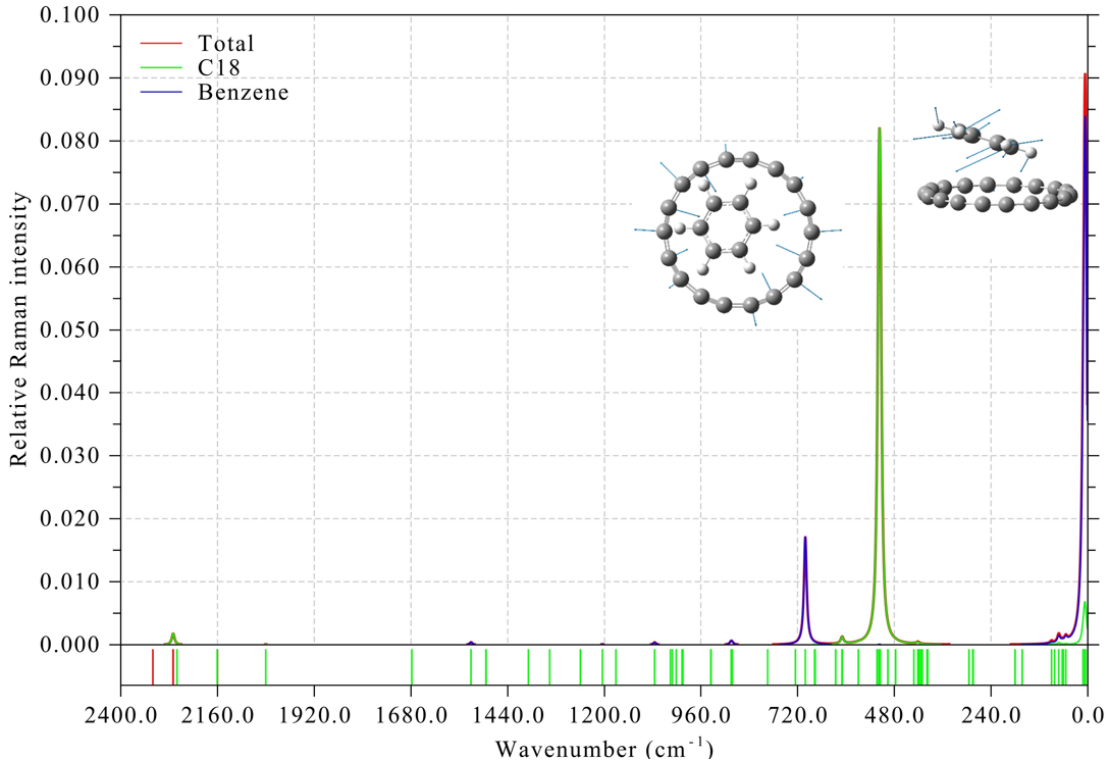

Fig.4 Simulated Raman spectrum of cyclo[18]carbon-benzene dimer with incident light at wavelength of 1064 nm,The red curve was broadened from calculated Raman intensities,The red and green spikes at bottom of the map indicate frequencies of in-plane and out-of-plane vibrational modes, respectively.

3.3 Orbital composition and Density-of-States(DOS)

The structure we calculated has 780 molecular orbitals, among them, there are 75 occupied molecular orbitals(MOs), These 75 MOs can be divided into two groups, namely 47 σ MOs and 28 π MOs, 25 of π MOs are provided by cyclo[18]carbon, The remaining three are provided by benzene ring. At the current calculation level, we found that the the energies of HOMO orbital(75th MO) and LUMO orbital(76th MO) of this structure are -8.69ev and -1.48ev, respectively. The corresponding HOMO-LUMO gap is 7.21ev, bigger than 6.75ev of cyclo[18]carbon HOMO-LUMO gap, this implies that cyclo[18]carbon-benzene dimer has poorer current conductivity than cyclo[18]carbon[35]. According to the following formula for calculating polarizability[36].

$$\alpha_{AB}(-\omega;\omega)=\sum_{i\neq 0}\left[\frac{\mu_{0i}^{A}\mu_{i0}^{B}}{\Delta_i-\omega}+\frac{\mu_{0i}^{B}\mu_{i0}^{A}}{\Delta_i+\omega}\right]=\hat{P}\left[A(-\omega),B(\omega)\right]\sum_{i\neq 0}\frac{\mu_{0i}^{A}\mu_{i0}^{B}}{\Delta_i-\omega}$$

cyclo[18]carbon has stronger polarizability than cyclo[18]carbon-benzene dimer[16], there is one term in the denominator is excitation energy, this is related to the energy difference between the two orbitals of dominant electron excitation, So if HOMO-LUMO gap is smaller, it means that the energy difference between occupied molecular orbitals and unoccupied molecular orbitals is smaller, furthermore, it can be known that excitation energy is smaller, ultimately, it can be inferred that polarizability is larger[36].

We analyze the contribution of atoms to the orbital composition of of the dimer using Hirshfeld method[37] by Multiwfn program in this paper, and lists the atomic composition of HOMO and LUMO orbitals in following table, third carbon atom has the greatest contribution to the HOMO orbit from Table.3, fourteenth carbon atom has the greatest contribution to the LUMO orbit from

Table.4, both of them belong to cyclo[18]carbon. As a whole, the contribution of cyclo[18]carbon to the HOMO orbit is 99.86%, the contribution of cyclo[18]carbon to the LUMO orbit is 99.45%, the contribution of benzene ring to the HOMO orbit is 0.14%, the contribution of benzene ring to the LUMO orbit is 0.55%.

Table 3 Atomic composition of HOMO

Atom	Proportion(%)	Atom	Proportion(%)	Atom	Proportion(%)
1C	9.011%	11C	1.304 %	21C	0.010 %
2C	6.013%	12C	3.431 %	22C	0.017 %
3C	10.248%	13C	1.190 %	23C	0.014 %
4C	8.904 %	14C	1.336 %	24C	0.014 %
5C	9.204 %	15C	3.060 %	25H	0.010 %
6C	10.241 %	16C	1.166 %	26H	0.016 %
7C	6.446 %	17C	6.126 %	27H	0.016 %
8C	9.299 %	18C	2.979 %	28H	0.011 %
9C	3.342 %	19C	0.017 %	29H	0.005 %
10C	6.557 %	20C	0.011 %	30H	0.005 %

Table 4 Atomic composition of LUMO

Atom	Proportion(%)	Atom	Proportion(%)	Atom	Proportion(%)
1C	2.629 %	11C	9.343 %	21C	0.026 %
2C	4.614 %	12C	7.799 %	22C	0.030 %
3C	1.290 %	13C	9.772 %	23C	0.015 %
4C	2.149 %	14C	9.651 %	24C	0.014 %
5C	1.883 %	15C	8.196 %	25H	0.063 %
6C	1.253 %	16C	9.548 %	26H	0.124 %
7C	4.160 %	17C	5.352 %	27H	0.123 %
8C	2.302 %	18C	7.537 %	28H	0.069 %
9C	7.104 %	19C	0.030 %	29H	0.010 %
10C	4.878 %	20C	0.027 %	30H	0.010 %

In addition, we also drew Overlap Population DOS(OPDOS)[38] map and Molecular Orbital Population DOS(MO-PDOS)[7] map of dimer, the positions of the dashed lines in Fig.5 and Fig.6 correspond to the HOMO orbit. From Fig.5, it can be seen that OPDOS presents a large negative value within the range of 0.20au to 1.10au energy, this means that these orbits will have an adverse impact on the combination of cyclo[18]carbon and benzene ring if these orbitals are occupied by electrons[38]. Namely antibonding. If we define the fragment in the OPDOS map as molecular orbital, we got MO-PDOS map, the graph can display the energy level positions of different orbits and their contributions to TDOS in Fig.6, it indicates the positions of σ MOs and π MOs and their contributions to TDOS.

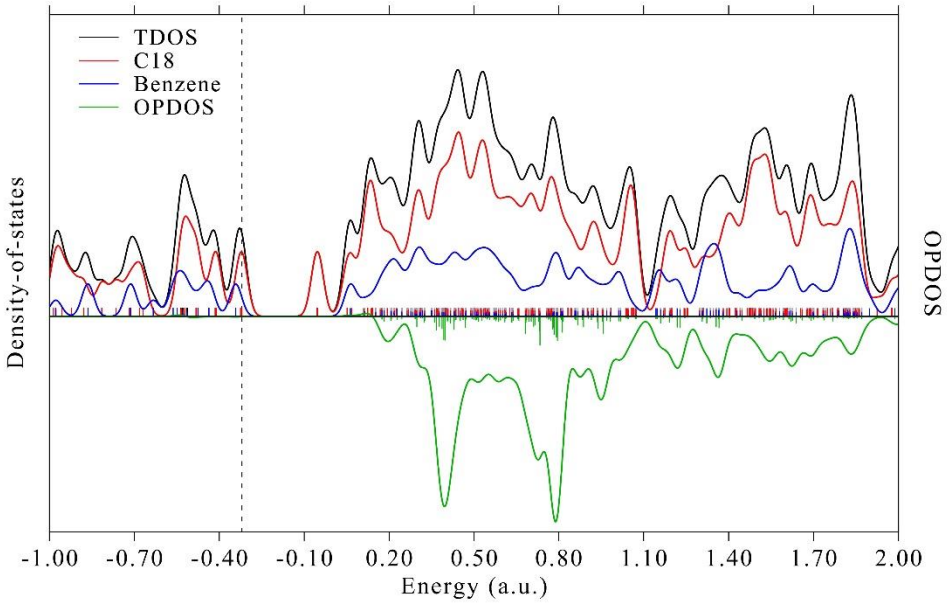

Fig.5 OPDOS map of cyclo[18]carbon-benzene dimer. Black curve corresponds to total DOS, while red, blue and green curves correspond to cyclo[18]carbon partial DOSs,benzene partial DOSs and Overlap population DOS, respectively. The dashed line represents the position of HOMO

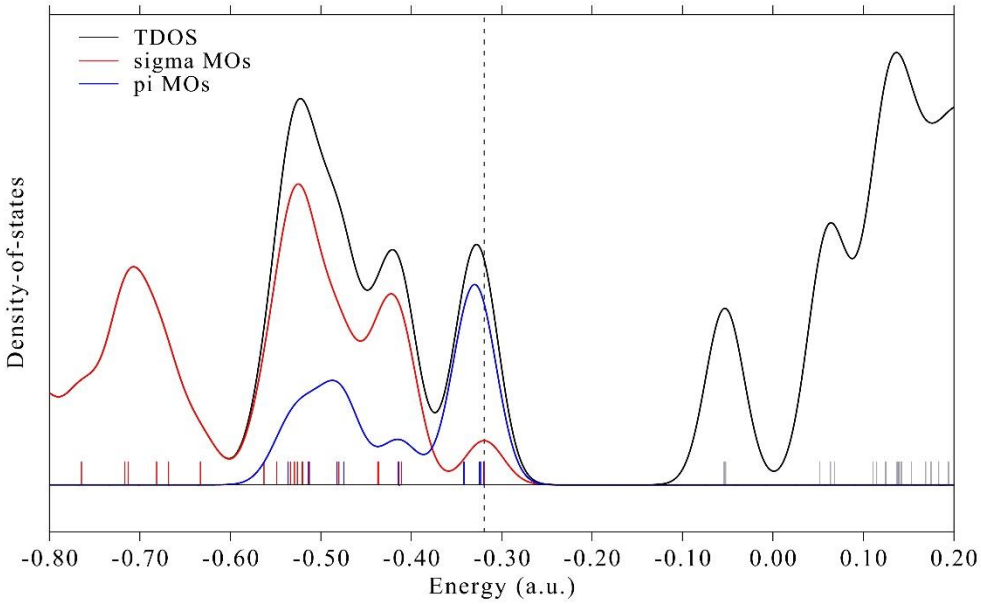

Fig.6 MO-PDOS map of cyclo[18]carbon-benzene dimer. Black curve corresponds to total DOS, while red and blue curves correspond to partial DOSs due to occupied σ Mos and π MOs, respectively,The dashed line represents the position of HOMO.

3.4 Weak interactions analysis

The optimized cyclo[18]carbon-benzene dimer lost symmetry compared to before optimization, it could explain by weak interactions analysis, previously, liu[35] studied the properties of cyclo[18]carbon dimer, they found a short C-C bond in one ring exactly faces a long C-C bond in another ring, they found that this question can be well answered according to the complementary principle of ESP[39], stacking in this manner can maximally minimize the electrostatic repulsion

caused by the unfavorable overlapping of the same sign of electrostatic potential(ESP) and ultimately lead to a minimum structure on the PES. So we drew the ESP map for cyclo[18]carbon-benzene dimer at Fig.7 and listed values of ESP at vdW surface in Table.5, further, we marked ESP maximum point and minimum point in the picture, yellow ball represents ESP maximum point, cyan ball represents ESP minimum point, the quantitative distribution of ESP is shown in the Fig.8. It can be seen that the surface area distribution inside different regions of ESP are extremely uneven, Fig.8 clearly displays that most regions of the vdW surface show positive ESP[42-43], and the areas of the positive and negative parts are calculated to be 222.7 and 118.4 Å^2, which occupy 65.3% and 34.7% of the entire vdW surface, respectively. So, from a pure electrostatic point of view, the cyclo[18]carbon will be more proned to combine with Lewis bases, instead of Lewis acids, it is because the magnitude of ESP maxima is larger than that of ESP minima on the vdW surface, and the area of the vdW surface with positive ESP is much larger than that with negative ESP.

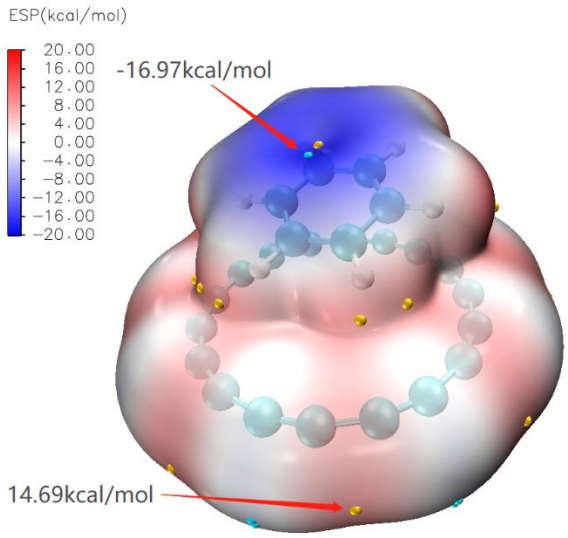

Fig.7 ESP mapped vdW surface (namely, isosurface of r ¼ 0.001 au) of the cyclo[18]carbon-benzene dimer. Minima and maxima of the ESP on the vdW surface are drawn as cyan and orange spheres, respectively, ESP maximum point is 14.69kcal/mol, ESP minimum point is -16.97kcal/mol

Table.5 Values of ESP at vdW surface

Number	surface minima(kcal/mol)	surface maxima(kcal/mol)
1	-2.149795	8.512777
2	-1.990166	8.363546
3	-1.527319	14.698076
4	1.344180	8.703631
5	-1.444687	14.105239
6	-2.143929	14.686497
7	-2.124730	8.544929
8	-0.983040	-16.673597
9	-1.776920	8.677471
10	-15.937406	9.931460
11	-16.933315	14.015553
12	-1.959212	-0.439031
13	-16.974593	10.106147

14	-1.527315	-0.472630
15	-1.704591	8.709280
16	-1.755866	9.852097
17	-1.699123	9.872591
18	-1.669108	9.830718
19	-1.692966	8.618512
20		8.667227
21		8.631592

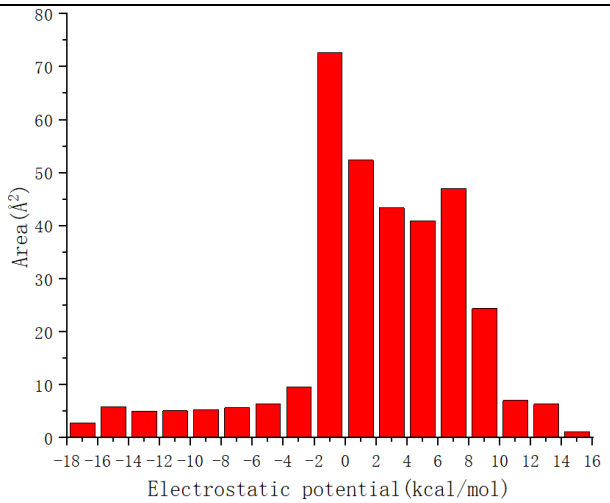

Fig.8 Area distribution of different ESP intervals.

To determine why a structure with such low symmetry can exist stably, based on the optimized structure, we were calculated interaction energy with counterpoise correction at the ωB97X-V/def2-QZVPP level. We know that its interaction energy is 15.59kcal/mol after calculation, which is not only bigger than six times that of the parallelly stacked benzene dimer(2.7kcal/mol)[44], even more than cyclo[18]carbon dimer(9.2kcal/mol)[35]. Obviously, the combination of cyclo[18]carbon and benzene ring is very strong. And then, we employed SAPT method to characterize the nature of intermolecular interaction by SAPT0[33] method with jun-cc-pVDZ basis, because the calculation cost of the SAPT2+(3)δMP2 method is prohibitively high for the cyclo[18]carbon-benzene dimer, this level can at least provide qualitatively meaningful result of various physical components for the study of intermolecular interactions. The results are shown in Table.6.

Table.6 Interaction components between cyclo[18]carbon and benzene ring in the dimer structure calculated at the scaled SAPT0/jun-cc-pVDZ level.

Component	Value(kcal/mol)
Exchange-repulsion	-2.9
Electrostatic	7.4
Induction	-0.6
Dispersion	-11.5
Total	-7.6

Finally, we plotted the interaction map for the cyclo[18]carbon-benzene dimer by interaction region indicator(IRI)[40], the method was proposed in 2021 and its definition is as following formula, where a is an adjustable parameter, IRI is essentially the gradient norm of electron density

weighted by scaled electron density. Compared to traditional method to showing weak interactions through graphic such as Noncovalent interaction(NCI)[41] method, IRI can perfectly and comprehensively showcase weak interactions in one picture, Fig.9 represents the coloring bar.

$$\mathrm{IRI\ (r)} = \frac{|\nabla\rho(r)|}{[\rho(r)]^a}$$

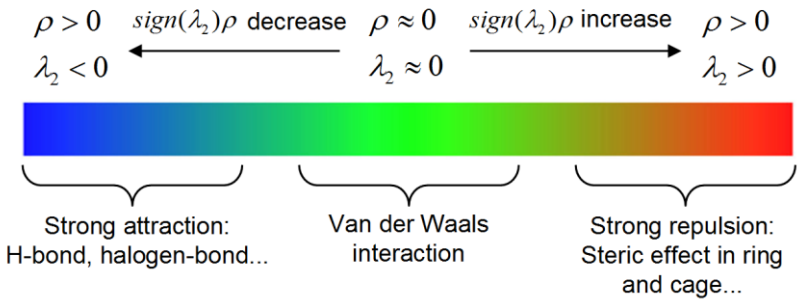

Fig.9 Standard coloring method and chemical explanation of sign(λ_2)ρ on IRI isosurfaces.

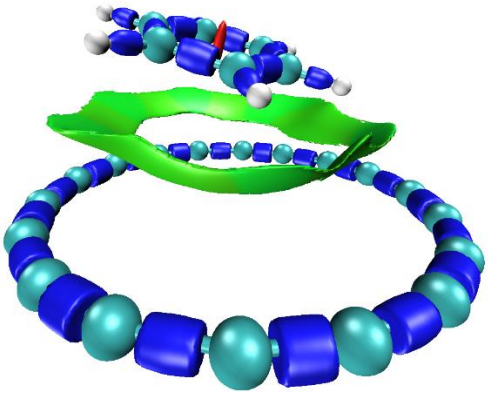

Fig.10 Optimized structures and IRI maps of cyclo[18]carbon-benzene dimer. The surfaces between the cyclo[18]carbon and the Benzene correspond to the isosurface of IRI (isovalue=1) mapped by sign(λ2)ρ function. The color scale is given in au

From the IRI diagram, it can be seen there is a strong vdW interaction (green area) between the benzene ring and the cyclo[18]carbon, this has been proved by the calculation of interaction energy above, due to the fact that the benzene ring is not parallel to the cyclo[18]carbon, the green area is not uniform.

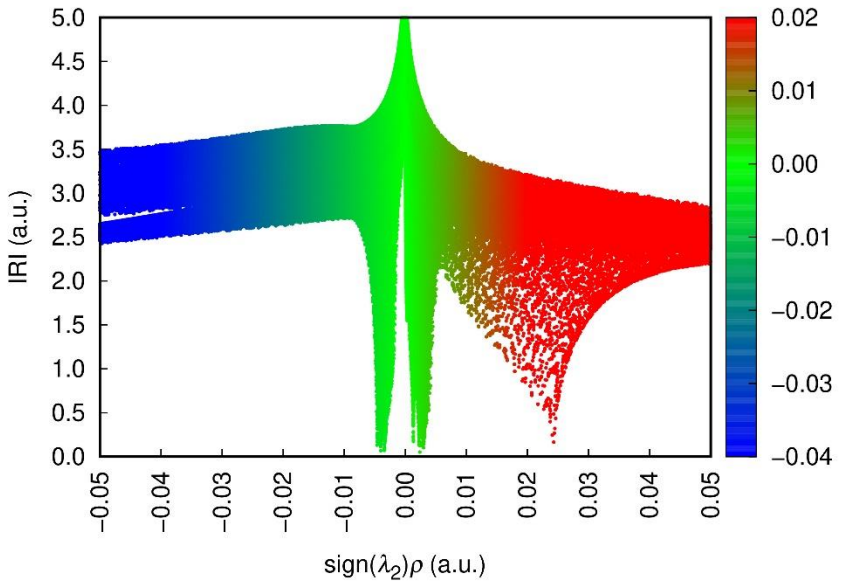

Fig.11 cyclo[18]carbon-benzene dimer IRI vs sign(λ2)ρ scatter graph

Fig.10 shows the IRI vs sign(λ2)ρ scatter graph of cyclo[18]carbon-benzene dimer, there are several spikes in the range of -0.01au to 0.01au, corresponds to the weak interaction between cyclo[18]carbon and benzene, and in the range of 0.02au to 0.03au, it corresponds to strong mutual exclusion.

3.5 Other molecular properties

Finally, we present a collection of frequently involved molecular properties for the cyclo[18]carbon-benzene dimer, calculated and label the total dipole moment of the system and the dipole moment of each monomer in Fig.12 by Multiwfn, radius and volume of cyclo[18]carbon in cyclo[18]carbon-benzene dimer in Table.7 and change in cyclo[18]carbon radius in Fig.13.

As shown in Fig.12, the values of the dipole moment of the cyclo[18]carbon-benzene dimer is -0.132788au, 0.069591au, 0.038788au, cyclo[18]carbon is -0.095873au, 0.050171au, 0.084854au, benzene ring is -0.036915au, 0.019420au, -0.046065au. Then we calculated sphericity of cyclo[18]carbon-benzene dimer and radius of cyclo[18]carbon by Multiwfn, the comparison of radii is shown in the Table.7, the difference between the two is 0.000614Å, and lastly, the sphericity of cyclo[18]carbon-benzene dimer is 0.7565, Greater than 0.7211 of cyclo[18]carbon.

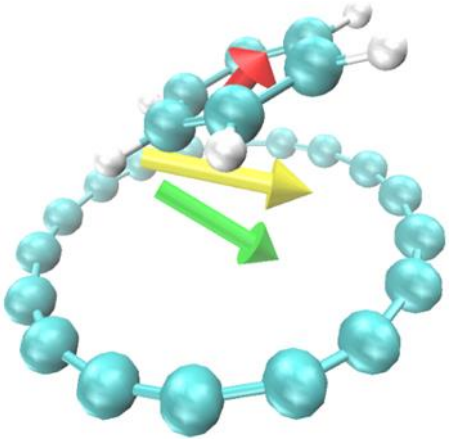

Fig.12 Molecular dipole moment diagram of cyclo[18]carbon-benzene, the yellow arrow represents the total dipole moment of system, The red and green arrow represents the dipole moment of benzene and cyclo[18]carbon

Table.7 Comparison of Radius, A represents cyclo[18]carbon, B represents cyclo[18]carbon in cyclo[18]carbon-benzene dimer

	Radius(Å)	Volume(Å^3)
A	1.992542	33.136829
B	1.993156	33.167478

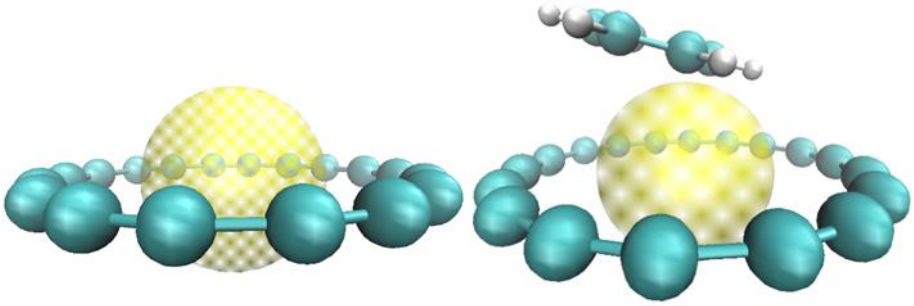

Fig.13 Diagram of radius for cyclo[18]carbon and cyclo[18]carbon in cyclo[18]carbon-benzene dimer

4. Conclusions

We conducted a systematic and depth theoretical exploration of interaction between cyclo[18]carbon and benzene ring, analyzed the structure of cyclo[18]carbon-benzene dimer by mayer bond order based on the result of geometry optimization, listed the changes in C-C bond of cyclo[18]carbon. The infrared and Raman spectra were drawn and several vibration modes of dimer were identified. Confirmed that cyclo[18]carbon-benzene dimer has 780 molecular orbital in total and composition of orbital, 75 of them have occupied, the values of HOMO, LUMO and HOMO-LUMO gap were obtained, implies that cyclo[18]carbon-benzene dimer has poorer current conductivity and larger polarizability than cyclo[18]carbon, determined the contribution of each atom to HOMO and LUMO， and cyclo[18]carbon has the more contribution to HOMO and LUMO than benzene ring. Drew Overlap Population DOS(OPDOS) map and Molecular Orbital Population DOS(MO-PDOS) map of dimer, discussed that if which orbitals are occupied, it will have adverse impact on the combination of cyclo[18]carbon and benzene ring. Further investigation was conducted on the causes of structural distortion after optimization of cyclo[18]carbon-benzene dimer by weak interactions analysis, then ESP mapped vdW surface (namely, isosurface of r ¼ 0.001 au) of the cyclo[18]carbon-benzene dimer. Listed all values of ESP and area distribution of different ESP intervals, calculated interaction components between cyclo[18]carbon and benzene ring in the dimer structure at the SAPT0/jun-cc-pVDZ level, graphical display of the interaction between cyclo[18]carbon and benzene ring by IRI method. Lastly, present a collection of frequently involved molecular properties for the dimer like dipole moment, sphericity and change of radius of cyclo[18]carbon. In summary, this article utilized ORCA with the assistance of a series of programs such as Multiwfn to study the structure composed of cyclo[18]carbon and benzenen ring, which is of positive significance for the exploration of cyclo[18]carbon, especially the interaction witn small molecules and the adsorption.

5. CRediT authorship contribution statement

Peng Fu: Writing - original draft, Funding acquisition, Visualization, Formal analysis.

6. Declaration of competing interest

The authors declare that they have no known competing financial interests or personal relationships that could have appeared to influence the work reported in this paper.

7. Reference

[1]Li, Y., Xu, L., Liu, H., Li, Y. Graphdiyne and graphyne: From theoretical predictions to practical construction[J]. Chem. Soc. Rev. 2014, 43: 2572-2586.

[2]Zhang, S., Zhou, J., Wang, Q., Chen, X., Kawazoe, Y., Jena, P. Penta-graphene: A new carbon allotrope[J]. PNAS. 2015, 112: 2372-2377.

[3]Sheng, X. L., Yan, Q. B., Ye, F., Zheng, Q. R., Su, G. T-carbon: a novel carbon allotrope[J]. Phys. Rev. Lett. 2011, 106: 155703.

[4]Zhang, J., Wang, R., Zhu, X., Pan, A., Han, C., Li, X., Dan, Z., Ma, C., Wang, W., Su, H., Niu, C. Pseudo-topotactic conversion of carbon nanotubes to T-carbon nanowires under picosecond laser irradiation in methanol[J]. Nat. Commun. 2017, 8: 683.

[5]T. Lu, Q. Chen, Z. Liu, A thorough theoretical exploration of intriguing characteristics of cyclo[18]carbon: geometry, bonding nature, aromaticity, weak interaction, reactivity, excited states, vibrations, molecular dynamics andvarious molecular properties, ChemRxiv (2019), https://doi.org/10.26434/chemrxiv.11320130.

[6]Liu Z, Lu T, Chen Q. An sp-hybridized all-carboatomic ring, cyclo [18] carbon: Electronic structure, electronic spectrum, and optical nonlinearity[J]. Carbon, 2020, 165: 461-467.

[7]Liu Z, Lu T, Chen Q. An sp-hybridized all-carboatomic ring, cyclo [18] carbon: Bonding character, electron delocalization, and aromaticity[J]. Carbon, 2020, 165: 468-475.

[8]Kaiser K, Scriven L M, Schulz F, et al. An sp-hybridized molecular carbon allotrope, cyclo [18] carbon[J]. Science, 2019, 365(6459): 1299-1301.

[9]Hoffmann R. Extended Hückel theory—V: Cumulenes, polyenes, polyacetylenes and Cn[J]. Tetrahedron, 1966, 22(2): 521-538.

[10]Shieh P, Hill M R, Zhang W, et al. Clip chemistry: diverse (bio)(macro) molecular and material function through breaking covalent bonds[J]. Chemical Reviews, 2021, 121(12): 7059-7121.

[11]Guo Q H, Qiu Y, Wang M X, et al. Aromatic hydrocarbon belts[J]. Nature chemistry, 2021, 13(5): 402-419.

[12]Fan Q, Yan L, Tripp M W, et al. Biphenylene network: A nonbenzenoid carbon allotrope[J]. Science, 2021, 372(6544): 852-856.

[13]Liu Z, Lu T, Chen Q. Vibrational Spectra and Molecular Vibrational Behaviors of All-Carboatomic Rings, cyclo [18] carbon and Its Analogues[J]. Chemistry–An Asian Journal, 2021, 16(1): 56-63.

[14]Lu T, Chen Q. Ultrastrong regulation effect of the electric field on the all-carboatomic ring cyclo [18] carbon[J]. ChemPhysChem, 2021, 22(4): 386-395.

[15]Liu Z, Lu T, Chen Q. Comment on “Theoretical investigation on bond and spectrum of cyclo [18] carbon (C18) with sp-hybridized”[J]. Journal of Molecular Modeling, 2021, 27(2): 42.

[16]Liu Z, Lu T, Yuan A, et al. Remarkable Size Effect on Photophysical and Nonlinear Optical Properties of All-Carboatomic Rings, Cyclo [18] carbon and Its Analogues[J]. Chemistry–An Asian Journal, 2021, 16(16): 2267-2271.

[17]Lu T, Liu Z, Chen Q. Comment on “18 and 12–Member carbon rings (cyclo [n] carbons)–A density functional study”[J]. Materials Science and Engineering: B, 2021, 273: 115425.

[18]Liu Z, Wang X, Lu T, et al. Potential optical molecular switch: Lithium@ cyclo [18] carbon complex transforming between two stable configurations[J]. Carbon, 2022, 187: 78-85.

[19]M.J. Frisch, G.W. Trucks, H.B. Schlegel, G.E. Scuseria, M.A. Robb,J.R. Cheeseman, et al., Gaussian 16, Revision A.03, Gaussian, Inc., Wallingford,CT, 2016.
[20]Neese F. Software update: the ORCA program system, version 4.0[J]. Wiley Interdisciplinary Reviews: Computational Molecular Science, 2018, 8(1): e1327.
[21]Neese, F.; Wennmohs, F.; Hansen, A.; Becker, U., Efficient, approximate and parallel Hartree–Fock and hybrid DFT calculations. A 'chain-of-spheres' algorithm for the Hartree–Fock exchange. Chem. Phys. 2009, 356 (1), 98-109.
[22]Izsák, R.; Neese, F., An overlap fitted chain of spheres exchange method. J. Chem. Phys. 2011, 135 (14), 144105.
[23]Izsák, R.; Neese, F.; Klopper, W., Robust fitting techniques in the chain of spheres approximation to the Fock exchange: The role of the complementary space. J. Chem. Phys. 2013, 139 (9), 094111.
[24]Helmich-Paris, B.; de Souza, B.; Neese, F.; Izsák, R., An improved chain of spheres for exchange algorithm. J. Chem. Phys. 2021, 155 (10), 104109.
[25]Lin Y S, Li G D, Mao S P, et al. Long-range corrected hybrid density functionals with improved dispersion corrections[J]. Journal of Chemical Theory and Computation, 2013, 9(1): 263-272.
[26]Weigend F, Ahlrichs R. Balanced basis sets of split valence, triple zeta valence and quadruple zeta valence quality for H to Rn: Design and assessment of accuracy[J]. Physical Chemistry Chemical Physics, 2005, 7(18): 3297-3305.
[27]Chai J D, Head-Gordon M. Long-range corrected hybrid density functionals with damped atom–atom dispersion corrections[J]. Physical Chemistry Chemical Physics, 2008, 10(44): 6615-6620.
[28]Schäfer A, Huber C, Ahlrichs R. Fully optimized contracted Gaussian basis sets of triple zeta valence quality for atoms Li to Kr[J]. The Journal of chemical physics, 1994, 100(8): 5829-5835.
[29]Mardirossian N, Head-Gordon M. ωB97X-V: A 10-parameter, range-separated hybrid, generalized gradient approximation density functional with nonlocal correlation, designed by a survival-of-the-fittest strategy[J]. Physical Chemistry Chemical Physics, 2014, 16(21): 9904-9924.
[30]Lu T, Chen F. Multiwfn: A multifunctional wavefunction analyzer[J]. Journal of computational chemistry, 2012, 33(5): 580-592.
[31]Mayer I. Charge, bond order and valence in the AB initio SCF theory[J]. Chemical Physics Letters, 1983, 97(3): 270-274.
[32]Parrish R M, Burns L A, Smith D G A, et al. Psi4 1.1: An open-source electronic structure program emphasizing automation, advanced libraries, and interoperability[J]. Journal of chemical theory and computation, 2017, 13(7): 3185-3197.
[33]Parker T M, Burns L A, Parrish R M, et al. Levels of symmetry adapted perturbation theory (SAPT). I. Efficiency and performance for interaction energies[J]. The Journal of chemical physics, 2014, 140(9): 094106.
[34]Alecu I M, Zheng J, Zhao Y, et al. Computational thermochemistry: scale factor databases and scale factors for vibrational frequencies obtained from electronic model chemistries[J]. Journal of chemical theory and computation, 2010, 6(9): 2872-2887.
[35]Liu Z, Lu T, Chen Q. Intermolecular interaction characteristics of the all-carboatomic ring, cyclo [18] carbon: Focusing on molecular adsorption and stacking[J]. Carbon, 2021, 171: 514-523.
[36]Sasagane K, Aiga F, Itoh R. Higher-order response theory based on the quasienergy derivatives: The derivation of the frequency-dependent polarizabilities and hyperpolarizabilities[J]. The Journal

of chemical physics, 1993, 99(5): 3738-3778.
[37]Spackman M A, Jayatilaka D. Hirshfeld surface analysis[J]. CrystEngComm, 2009, 11(1): 19-32.
[38]Bultinck P, Van Alsenoy C, Ayers P W, et al. Critical analysis and extension of the Hirshfeld atoms in molecules[J]. The Journal of chemical physics, 2007, 126(14): 144111.
[39]Lu T, Chen F. Revealing the nature of intermolecular interaction and configurational preference of the nonpolar molecular dimers (H 2) 2,(N 2) 2, and (H 2)(N 2)[J]. Journal of molecular modeling, 2013, 19: 5387-5395.
[40]Lu T, Chen Q. Interaction region indicator: A simple real space function clearly revealing both chemical bonds and weak interactions[J]. Chemistry-Methods, 2021, 1(5): 231-239.
[41]Johnson E R, Keinan S, Mori-Sánchez P, et al. Revealing noncovalent interactions[J]. Journal of the American Chemical Society, 2010, 132(18): 6498-6506.
[42]Manzetti S, Lu T. The geometry and electronic structure of Aristolochic acid: possible implications for a frozen resonance[J]. Journal of Physical Organic Chemistry, 2013, 26(6): 473-483.
[43]Lu T, Manzetti S. Wavefunction and reactivity study of benzo [a] pyrene diol epoxide and its enantiomeric forms[J]. Structural Chemistry, 2014, 25: 1521-1533.
[44] Rezác J, Riley K E, Hobza P. Extensions of the S66 data set: more accurate interaction energies and angular-displaced nonequilibrium geometries[J]. Journal of Chemical Theory and Computation, 2011, 7(11): 3466-3470.